Search for Correlations of High-energy Neutrinos Detected in IceCube with Radio-bright AGN and Gamma-Ray Emission from Blazars

R. Abbasi[1], M. Ackermann[2], J. Adams[3], S. K. Agarwalla[4,65], J. A. Aguilar[5], M. Ahlers[6], J. M. Alameddine[7],
N. M. Amin[8], K. Andeen[9], G. Anton[10], C. Argüelles[11], Y. Ashida[4], S. Athanasiadou[2], S. N. Axani[8], X. Bai[12],
A. Balagopal V.[4], M. Baricevic[4], S. W. Barwick[13], V. Basu[4], R. Bay[14], J. J. Beatty[15,16], K.-H. Becker[17],
J. Becker Tjus[18,66], J. Beise[19], C. Bellenghi[20], C. Benning[21], S. BenZvi[22], D. Berley[23], E. Bernardini[24],
D. Z. Besson[25], G. Binder[14,26], E. Blaufuss[23], S. Blot[2], F. Bontempo[27], J. Y. Book[11], C. Boscolo Meneguolo[24],
S. Böser[28], O. Botner[19], J. Böttcher[21], E. Bourbeau[6], J. Braun[4], B. Brinson[29], J. Brostean-Kaiser[2], R. T. Burley[30],
R. S. Busse[31], D. Butterfield[4], M. A. Campana[32], K. Carloni[11], E. G. Carnie-Bronca[30], S. Chattopadhyay[4,67], N. Chau[5],
C. Chen[29], Z. Chen[33], D. Chirkin[4], S. Choi[34], B. A. Clark[23], L. Classen[31], A. Coleman[19], G. H. Collin[35],
A. Connolly[15,16], J. M. Conrad[35], P. Coppin[36], P. Correa[36], S. Countryman[37], D. F. Cowen[38,39], P. Dave[29],
C. De Clercq[36], J. J. DeLaunay[40], D. Delgado[11], H. Dembinski[8], S. Deng[21], K. Deoskar[41], A. Desai[4], P. Desiati[4],
K. D. de Vries[36], G. de Wasseige[42], T. DeYoung[43], A. Diaz[35], J. C. Díaz-Vélez[4], M. Dittmer[31], A. Domi[10],
H. Dujmovic[4], M. A. DuVernois[4], T. Ehrhardt[28], P. Eller[20], S. El Mentawi[21], R. Engel[27,44], H. Erpenbeck[4], J. Evans[23],
P. A. Evenson[8], K. L. Fan[23], K. Fang[4], K. Farrag[45], A. R. Fazely[46], A. Fedynitch[47], N. Feigl[48], S. Fiedlschuster[10],
C. Finley[41], L. Fischer[2], D. Fox[38], A. Franckowiak[18], E. Friedman[23], A. Fritz[28], P. Fürst[21], T. K. Gaisser[8],
J. Gallagher[49], E. Ganster[21], A. Garcia[11], L. Gerhardt[26], A. Ghadimi[40], C. Glaser[19], T. Glauch[20],
T. Glüsenkamp[10,19], N. Goehlke[44], J. G. Gonzalez[8], S. Goswami[40], D. Grant[43], S. J. Gray[23], O. Gries[21], S. Griffin[4],
S. Griswold[22], C. Günther[21], P. Gutjahr[7], C. Haack[20], A. Hallgren[19], R. Halliday[43], L. Halve[21], F. Halzen[4],
H. Hamdaoui[33], M. Ha Minh[20], K. Hanson[4], J. Hardin[35], A. A. Harnisch[43], P. Hatch[50], A. Haungs[27], K. Helbing[17],
J. Hellrung[18], F. Henningsen[20], L. Heuermann[21], N. Heyer[19], S. Hickford[17], A. Hidvegi[41], C. Hill[45], G. C. Hill[30],
K. D. Hoffman[23], S. Hori[4], K. Hoshina[4,68], W. Hou[27], T. Huber[27], K. Hultqvist[41], M. Hünnefeld[7], R. Hussain[4],
K. Hymon[7], S. In[34], A. Ishihara[45], M. Jacquart[4], O. Janik[21], M. Jansson[41], G. S. Japaridze[51], K. Jayakumar[4,69], M. Jeong[34],
M. Jin[11], B. J. P. Jones[52], D. Kang[27], W. Kang[34], X. Kang[32], A. Kappes[31], D. Kappesser[28], L. Kardum[7], T. Karg[2],
M. Karl[20], A. Karle[4], U. Katz[10], M. Kauer[4], J. L. Kelley[4], A. Khatee Zathul[4], A. Kheirandish[53,54],
J. Kiryluk[33], S. R. Klein[14,26], A. Kochocki[43], R. Koirala[8], H. Kolanoski[48], T. Kontrimas[20], L. Köpke[28],
C. Kopper[10,43], D. J. Koskinen[6], P. Koundal[27], M. Kovacevich[32], M. Kowalski[2,48], T. Kozynets[6], K. Kruiswijk[42],
E. Krupczak[43], A. Kumar[2], E. Kun[18], N. Kurahashi[32], N. Lad[2], C. Lagunas Gualda[2], M. Lamoureux[42],
M. J. Larson[23], S. Latseva[21], F. Lauber[17], J. P. Lazar[4,11], J. W. Lee[34], K. Leonard DeHolton[38,39],
A. Leszczyńska[8], M. Lincetto[18], Q. R. Liu[4], M. Liubarska[55], E. Lohfink[28], C. Love[32], C. J. Lozano Mariscal[31],
L. Lu[4], F. Lucarelli[56], A. Ludwig[57], W. Luszczak[15,16], Y. Lyu[14,26], J. Madsen[4], K. B. M. Mahn[43], Y. Makino[4],
E. Manao[20], S. Mancina[4,24], W. Marie Sainte[4], I. C. Mariş[5], S. Marka[37], Z. Marka[37], M. Marsee[40], I. Martinez-Soler[11],
R. Maruyama[58], F. Mayhew[43], T. McElroy[55], F. McNally[59], J. V. Mead[6], K. Meagher[4], S. Mechbal[2], A. Medina[16],
M. Meier[45], Y. Merckx[36], L. Merten[18], J. Micallef[43], T. Montaruli[56], R. W. Moore[55], Y. Morii[45], R. Morse[4],
M. Moulai[4], T. Mukherjee[27], R. Naab[2], R. Nagai[45], M. Nakos[4], U. Naumann[17], J. Necker[2], M. Neumann[31],
H. Niederhausen[43], M. U. Nisa[43], A. Noell[21], S. C. Nowicki[43], A. Obertacke Pollmann[45], V. O'Dell[4], M. Oehler[27],
B. Oeyen[60], A. Olivas[23], R. Orsoe[20], J. Osborn[4], E. O'Sullivan[19], H. Pandya[8], N. Park[50], G. K. Parker[52],
E. N. Paudel[8], L. Paul[9], C. Pérez de los Heros[19], J. Peterson[4], S. Philippen[21], S. Pieper[17], A. Pizzuto[4], M. Plum[12],
A. Pontén[19], Y. Popovych[28], M. Prado Rodriguez[4], B. Pries[43], R. Procter-Murphy[23], G. T. Przybylski[26], J. Rack-Helleis[28],
K. Rawlins[61], Z. Rechav[4], A. Rehman[8], P. Reichherzer[18], G. Renzi[5], E. Resconi[20], S. Reusch[2], W. Rhode[7],
M. Richman[32], B. Riedel[4], A. Rifaie[21], E. J. Roberts[30], S. Robertson[14,26], S. Rodan[34], G. Roellinghoff[34], M. Rongen[10],
C. Rott[34,62], T. Ruhe[7], L. Ruohan[20], D. Ryckbosch[60], I. Safa[4,11], J. Saffer[44], D. Salazar-Gallegos[43],
P. Sampathkumar[27], S. E. Sanchez Herrera[43], A. Sandrock[17], M. Santander[40], S. Sarkar[55], S. Sarkar[63], J. Savelberg[21],
P. Savina[4], M. Schaufel[21], H. Schieler[27], S. Schindler[10], L. Schlickmann[21], B. Schlüter[31], F. Schlüter[5], T. Schmidt[23],
J. Schneider[10], F. G. Schröder[8,27], L. Schumacher[20], G. Schwefer[21], S. Sclafani[32], D. Seckel[8], M. Seikh[25],
S. Seunarine[64], R. Shah[32], A. Sharma[19], S. Shefali[44], N. Shimizu[45], M. Silva[4], B. Skrzypek[11], B. Smithers[52],
R. Snihur[4], J. Soedingrekso[7], A. Søgaard[6], D. Soldin[44], P. Soldin[21], G. Sommani[18], C. Spannfellner[20],
G. M. Spiczak[64], C. Spiering[2], M. Stamatikos[16], T. Stanev[8], T. Stezelberger[26], T. Stürwald[17], T. Stuttard[6],
G. W. Sullivan[23], I. Taboada[29], S. Ter-Antonyan[46], M. Thiesmeyer[21], W. G. Thompson[11], J. Thwaites[4], S. Tilav[8],
K. Tollefson[43], C. Tönnis[34], S. Toscano[5], D. Tosi[4], A. Trettin[2], C. F. Tung[29], R. Turcotte[27], J. P. Twagirayezu[43],
B. Ty[4], M. A. Unland Elorrieta[31], A. K. Upadhyay[4,70], K. Upshaw[46], N. Valtonen-Mattila[19], J. Vandenbroucke[4],
N. van Eijndhoven[36], D. Vannerom[35], J. van Santen[2], J. Vara[31], J. Veitch-Michaelis[4], M. Venugopal[27], M. Vereecken[42],

S. Verpoest[60], D. Veske[37], C. Walck[41], T. B. Watson[52], C. Weaver[43], P. Weigel[35], A. Weindl[27], J. Weldert[38,39],
C. Wendt[4], J. Werthebach[7], M. Weyrauch[27], N. Whitehorn[43,57], C. H. Wiebusch[21], N. Willey[43], D. R. Williams[40],
A. Wolf[21], M. Wolf[20], G. Wrede[10], X. W. Xu[46], J. P. Yanez[55], E. Yildizci[4], S. Yoshida[45], R. Young[25], F. Yu[11], S. Yu[43],
T. Yuan[4], Z. Zhang[33], and P. Zhelnin[11]

IceCube Collaboration[71]

[1] Department of Physics, Loyola University Chicago, Chicago, IL 60660, USA
[2] Deutsches Elektronen-Synchrotron DESY, Platanenallee 6, D-15738 Zeuthen, Germany
[3] Department of Physics and Astronomy, University of Canterbury, Private Bag 4800, Christchurch, New Zealand
[4] Department of Physics and Wisconsin IceCube Particle Astrophysics Center, University of Wisconsin–Madison, Madison, WI 53706, USA
[5] Université Libre de Bruxelles, Science Faculty CP230, B-1050 Brussels, Belgium
[6] Niels Bohr Institute, University of Copenhagen, DK-2100 Copenhagen, Denmark
[7] Department of Physics, TU Dortmund University, D-44221 Dortmund, Germany
[8] Bartol Research Institute and Department of Physics and Astronomy, University of Delaware, Newark, DE 19716, USA
[9] Department of Physics, Marquette University, Milwaukee, WI, 53201, USA
[10] Erlangen Centre for Astroparticle Physics, Friedrich-Alexander-Universität Erlangen-Nürnberg, D-91058 Erlangen, Germany
[11] Department of Physics and Laboratory for Particle Physics and Cosmology, Harvard University, Cambridge, MA 02138, USA
[12] Physics Department, South Dakota School of Mines and Technology, Rapid City, SD 57701, USA
[13] Department of Physics and Astronomy, University of California, Irvine, CA 92697, USA
[14] Department of Physics, University of California, Berkeley, CA 94720, USA
[15] Department of Astronomy, Ohio State University, Columbus, OH 43210, USA
[16] Department of Physics and Center for Cosmology and Astro-Particle Physics, Ohio State University, Columbus, OH 43210, USA
[17] Department of Physics, University of Wuppertal, D-42119 Wuppertal, Germany
[18] Fakultät für Physik & Astronomie, Ruhr-Universität Bochum, D-44780 Bochum, Germany
[19] Department of Physics and Astronomy, Uppsala University, Box 516, SE-75120 Uppsala, Sweden
[20] Physik-department, Technische Universität München, D-85748 Garching, Germany
[21] III. Physikalisches Institut, RWTH Aachen University, D-52056 Aachen, Germany
[22] Department of Physics and Astronomy, University of Rochester, Rochester, NY 14627, USA
[23] Department of Physics, University of Maryland, College Park, MD 20742, USA
[24] Dipartimento di Fisica e Astronomia Galileo Galilei, Università Degli Studi di Padova, I-35122 Padova PD, Italy
[25] Department of Physics and Astronomy, University of Kansas, Lawrence, KS 66045, USA
[26] Lawrence Berkeley National Laboratory, Berkeley, CA 94720, USA
[27] Karlsruhe Institute of Technology, Institute for Astroparticle Physics, D-76021 Karlsruhe, Germany
[28] Institute of Physics, University of Mainz, Staudinger Weg 7, D-55099 Mainz, Germany
[29] School of Physics and Center for Relativistic Astrophysics, Georgia Institute of Technology, Atlanta, GA 30332, USA
[30] Department of Physics, University of Adelaide, Adelaide, 5005, Australia
[31] Institut für Kernphysik, Westfälische Wilhelms-Universität Münster, D-48149 Münster, Germany
[32] Department of Physics, Drexel University, 3141 Chestnut Street, Philadelphia, PA 19104, USA
[33] Department of Physics and Astronomy, Stony Brook University, Stony Brook, NY 11794-3800, USA
[34] Department of Physics, Sungkyunkwan University, Suwon 16419, Republic of Korea
[35] Department of Physics, Massachusetts Institute of Technology, Cambridge, MA 02139, USA
[36] Vrije Universiteit Brussel (VUB), Dienst ELEM, B-1050 Brussels, Belgium
[37] Columbia Astrophysics and Nevis Laboratories, Columbia University, New York, NY 10027, USA
[38] Department of Astronomy and Astrophysics, Pennsylvania State University, University Park, PA 16802, USA
[39] Department of Physics, Pennsylvania State University, University Park, PA 16802, USA
[40] Department of Physics and Astronomy, University of Alabama, Tuscaloosa, AL 35487, USA
[41] Oskar Klein Centre and Department of Physics, Stockholm University, SE-10691 Stockholm, Sweden
[42] Centre for Cosmology, Particle Physics and Phenomenology—CP3, Université catholique de Louvain, Louvain-la-Neuve, Belgium
[43] Department of Physics and Astronomy, Michigan State University, East Lansing, MI 48824, USA
[44] Karlsruhe Institute of Technology, Institute of Experimental Particle Physics, D-76021 Karlsruhe, Germany
[45] Department of Physics and The International Center for Hadron Astrophysics, Chiba University, Chiba 263-8522, Japan
[46] Department of Physics, Southern University, Baton Rouge, LA 70813, USA
[47] Institute of Physics, Academia Sinica, Taipei, 11529, Taiwan
[48] Institut für Physik, Humboldt-Universität zu Berlin, D-12489 Berlin, Germany
[49] Department of Astronomy, University of Wisconsin–Madison, Madison, WI 53706, USA
[50] Department of Physics, Engineering Physics, and Astronomy, Queen's University, Kingston, ON K7L 3N6, Canada
[51] CTSPS, Clark-Atlanta University, Atlanta, GA 30314, USA
[52] Department of Physics, University of Texas at Arlington, 502 Yates Street, Science Hall Rm 108, Box 19059, Arlington, TX 76019, USA
[53] Department of Physics & Astronomy, University of Nevada, Las Vegas, NV, 89154, USA
[54] Nevada Center for Astrophysics, University of Nevada, Las Vegas, NV 89154, USA
[55] Department of Physics, University of Alberta, Edmonton, Alberta, Canada T6G 2E1, Canada
[56] Département de physique nucléaire et corpusculaire, Université de Genève, CH-1211 Genève, Switzerland
[57] Department of Physics and Astronomy, UCLA, Los Angeles, CA 90095, USA
[58] Department of Physics, Yale University, New Haven, CT 06520, USA
[59] Department of Physics, Mercer University, Macon, GA 31207-0001, USA
[60] Department of Physics and Astronomy, University of Gent, B-9000 Gent, Belgium
[61] Department of Physics and Astronomy, University of Alaska Anchorage, 3211 Providence Drive, Anchorage, AK 99508, USA
[62] Department of Physics and Astronomy, University of Utah, Salt Lake City, UT 84112, USA
[63] Department of Physics, University of Oxford, Parks Road, Oxford OX1 3PU, UK

[64] Department of Physics, University of Wisconsin, River Falls, WI 54022, USA

Abstract

The IceCube Neutrino Observatory sends realtime neutrino alerts with a high probability of being astrophysical in origin. We present a new method to correlate these events and possible candidate sources using 2089 blazars from the Fermi-LAT 4LAC-DR2 catalog and with 3413 active galactic nuclei (AGNs) from the Radio Fundamental Catalog. No statistically significant neutrino emission was found in any of the catalog searches. The result suggests that a small fraction, $<1\%$, of the studied AGNs emit neutrinos that pass the alert criteria, and is compatible with prior evidence for neutrino emission presented by IceCube and other authors from sources such as TXS 0506 + 056 and PKS 1502 + 106. We also present cross-checks to other analyses that claim a significant correlation using similar data samples.

Unified Astronomy Thesaurus concepts: Neutrino astronomy (1100); Gamma-ray sources (633); Radio active galactic nuclei (2134)

1. Introduction

Astrophysical neutrinos are weakly interacting, electrically neutral particles capable of revealing the origin of cosmic rays. Thought to be produced in regions near some of the most high-energy events in the universe, astrophysical neutrinos travel undeflected by magnetic fields delivering information relating to their original production mechanism. One example of these regions is NGC 1068, an active galactic nucleus (AGN), from which evidence of high-energy neutrino emission was recently found with the IceCube Neutrino Observatory (Abbasi et al. 2022a).

Despite ongoing research, the origins of astrophysical neutrinos remain largely unknown. However, AGNs are among the most promising candidate sources (Abbasi et al. 2022a, 2022b; Murase & Stecker 2022). In particular, blazars —AGNs that have jets pointing toward Earth—are thought to be likely sources. Recently, evidence has emerged of a spatial and temporal correlation with the emission from blazar TXS 0506 + 056 and the high-energy neutrino event IC170922A, detected by IceCube (Aartsen et al. 2018b). An alert was sent to other observatories and a follow-up campaign in multiple wavelengths was started. At the moment of neutrino detection, the blazar was flaring in gamma-rays, and it was determined that the chance of accidental coincidence was at the 3σ level. Subsequent retrospective analyses from the IceCube collaboration found an excess in neutrino events with respect to the expected atmospheric background coincident with the position of TXS 0506 + 056, with a significance at the 3.5σ level (Aartsen et al. 2018a). Later studies have also indicated a possible correlation between the blazar PKS 1502 + 106 and the IceCube neutrino event IC190730A (Oikonomou et al. 2021; Rodrigues et al. 2021).

Both IC170922A and IC190730A were high-energy neutrino events with a high probability of being astrophysical in origin. For each of these events, IceCube released public realtime "neutrino alerts." For an alert to be issued, the event must have passed at least one of several filtering streams based on its reconstructed energy and direction (Aartsen et al. 2017b; Blaufuss et al. 2019). These alerts can be used to search for correlations between different candidate sources, as other studies have shown, e.g., a search for correlations with radio-selected AGNs in Plavin et al. (2020) and with blazars in Giommi et al. (2020).

In this paper we develop a method to perform correlation analyses using the latest catalog of alerts that IceCube has published, IceCat-1 (Abbasi et al. 2023),[72] and various catalogs of candidate sources. These analyses also use different weighting schemes for the sources to account for different neutrino production mechanisms. As a use case, we present three analyses: two using blazars from Fermi 4LAC-DR2 catalog and one with AGNs from the RFC 2022a catalog. The paper is organized as follows: in Section 2 the IceCube Neutrino Observatory is introduced, in Section 3 the neutrino catalog and the two source catalogs considered for this paper are discussed, and in Section 4 we introduce the analysis technique. In Section 5 the results are provided. Section 6 contains the conclusion and a comparison to previous analyses that used similar samples.

2. The IceCube Neutrino Observatory

The IceCube Neutrino Observatory is a cubic-kilometer detector located at the South Pole (Aartsen et al. 2017a). It is a 3D array of 5160 Digital Optical Modules (DOMs) deployed along strings between depths of 1450 m and 2450 m below the ice. Each DOM contains a photomultiplier tube (Abbasi et al. 2010) and readout electronics (Abbasi et al. 2009). The array of DOMs detects neutrinos indirectly via the Cherenkov radiation produced by the relativistic charged particles that result from the interactions of neutrinos in the ice or bedrock below IceCube. The analyses presented in this paper are focused on track-like events, produced by charged-current muon–neutrino interactions.

---

[65] also at Institute of Physics, Sachivalaya Marg, Sainik School Post, Bhubaneswar 751005, India.
[66] also at Department of Space, Earth and Environment, Chalmers University of Technology, SE-412 96 Gothenburg, Sweden.
[67] also at Institute of Physics, Sachivalaya Marg, Sainik School Post, Bhubaneswar 751005, India.
[68] also at Earthquake Research Institute, University of Tokyo, Bunkyo, Tokyo 113-0032, Japan.
[69] also at Institute of Physics, Sachivalaya Marg, Sainik School Post, Bhubaneswar 751005, India.
[70] also at Institute of Physics, Sachivalaya Marg, Sainik School Post, Bhubaneswar 751005, India.
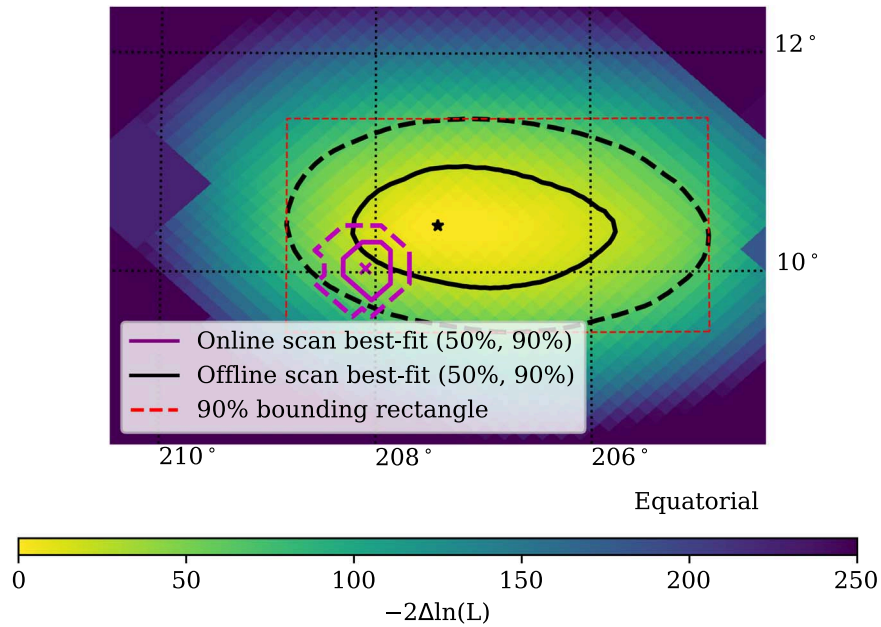[71] analysis@icecube.wisc.edu

Figure 1. Example of a log-likelihood map of a neutrino alert reconstructed with the full-sky maximum likelihood reconstruction algorithm in R.A. and decl. The black star is the best-fit position from the likelihood scan. The solid and dashed black curves represent the 50% and 90% confidence level, respectively, derived from the likelihood scan. The red dashed rectangle determines the errors quoted in the GCN Circulars and is defined as the minimum rectangle that would encapsulate the uncertainty contours. Lastly, the purple solid and dashed curves are the 50% and 90% confidence level contours calculated with the initial, less-refined reconstruction method and sent out in the first GCN Notice.

3. Data Samples

3.1. IceCube's Neutrino Alert Catalog

The IceCube Realtime System was established in 2016 (Aartsen et al. 2017b). Recently, the selection criteria were updated (Blaufuss et al. 2019), and now it consists of two alert streams, "Gold" and "Bronze" neutrino alerts, which are defined by an average astrophysical purity (signalness) of 50% and 30%, respectively. The signalness is calculated as the ratio between the expected number of astrophysical signal events and the expected total number of signal and background events with energy larger than the energy of the event and at the given decl. The expected number of signal events is calculated assuming a spectral index of 2.19 ± 0.10 (Haack & Wiebusch 2017) for the signal neutrino flux. The latest diffuse astrophysical muon–neutrino spectrum measured by IceCube has an index of 2.37 ± 0.09 (Abbasi et al. 2022c), but the signalness definition is kept unchanged for consistency. Typically, alert events have reconstructed neutrino energies above 100 TeV.

When IceCube detects a high-energy neutrino that passes the alert criteria, an automatic GCN[73] Notice is sent out to other observatories to allow for follow-up observations in multiple wavelength bands. This first notice contains the reconstructed direction with statistical uncertainties calculated with a fast reconstruction algorithm (Abbasi et al. 2021a). Another, more sophisticated reconstruction algorithm is then run and a second, updated GCN Notice and a GCN Circular are sent out a few hours later, including the refined reconstructed direction and uncertainties that also include systematic uncertainties.

This second algorithm is a maximum likelihood reconstruction method (Aartsen et al. 2014) that determines the neutrino

direction by running the track reconstruction for each direction (θ, ϕ) on an HEALPix (Gorski et al. 2005) grid covering the sky, with iteratively finer binning. The likelihood is calculated at every point of the grid, and the direction maximizing the likelihood represents the track whose light yield matches the observed data and therefore is used as the reconstructed direction of the neutrino. This likelihood map can be normalized to act as a spatial probability density function (PDF) for the neutrino (Figure 1). From the map, one can also derive uncertainty contours following the procedure explained in Abbasi et al. (2021b), in which an event is simulated and reconstructed multiple times to determine the appropriate confidence level and to account for systematic uncertainties. In practice, all of the events published in the realtime alert system in IceCube are calibrated using the simulations of one archival event, IC160427A. The work presented in Abbasi et al. (2021b) indicates that this method has difficulties in correctly accounting for systematic uncertainties and leads to a possible overcoverage of the angular resolution.

The IceCube Event Catalog of Alert Tracks-1 (IceCat-1; Abbasi et al. 2023) includes all of the alerts that were issued with the revised criteria as well as archival data starting from 2011, prior to the start of the realtime stream, which would have been selected as realtime alerts and were processed in the same way. In total, it contains 275 track-like events. Abbasi et al. (2023) also showed a simple correlation analysis searching for spatial coincidences between neutrino alerts and different candidate sources. The correlation analysis presented here represents an updated method with increased sensitivity to potential signal, since it includes additional information of the alert event and the candidate counterpart. In Figure 2, the spatial distribution of the alerts is shown, with the colors representing the signalness ratios of each event.

---

[73] General Coordinates Network, https://gcn.nasa.gov.
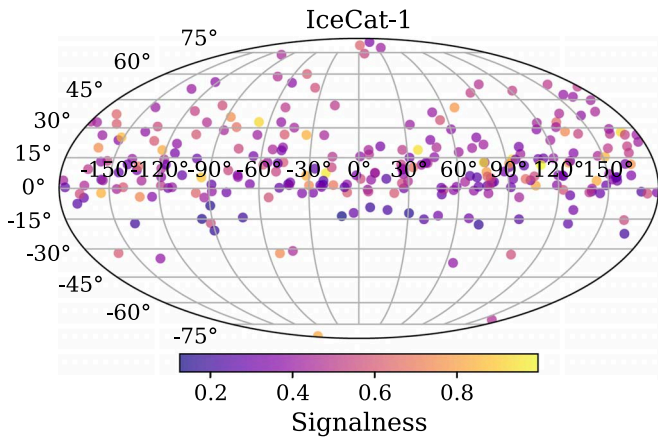
Figure 2. Neutrino events that have passed the alert criteria in the period between 2011 and 2020, in equatorial coordinates. The colors represent the probability that the neutrino is of astrophysical origin (signalness). The varying density in the number of events reflects the dependence of IceCube's effective area on the decl. of the neutrino direction.

3.2. Fermi-LAT Sources

For the first two analyses, blazars were selected from the incremental version of the Fourth Catalog of Active Galactic Nuclei detected by Fermi-LAT (4LAC-DR2, for Data Release 2; Ajello et al. 2020; Lott et al. 2020). This catalog contains all AGNs detected by Fermi-LAT between 2008 and 2018 at high galactic latitudes b ($|b| > 10°$). We select blazars (BL-Lacs, Flat Spectrum Radio Quasars and blazar candidates of unknown types), which represent 98% of the catalog.

The catalog was further refined by studying the distribution of sources in the sky to assure that it is isotropic, which fulfills the condition of isotropy that goes into the definition of the test statistic (TS), explained in Section 4. Various selection criteria with increasing limits on the brightness were applied to the gamma-ray energy flux F, which is defined as the energy flux of photons of a certain energy per unit area, $F = (dN/dEdAdt)E^2$, and obtained by spectral fitting from 100 MeV to 100 GeV. The latitude and longitude distributions of the blazar data after the selection were compared to a uniform distribution, both weighted by the energy flux and unweighted. A cut of $F \geqslant 10^{-11.6}$ erg cm^{-2} s^{-1} was chosen based on the results retaining 90% of the cumulative flux from all objects in the catalog. The final number of blazars used in the analysis is 2089 (from the original 3063 blazars in 4LAC-DR2).

Two weighting schemes are used in analyzing the 4LAC-DR2 catalog. For the first, the normalized 10 yr average energy flux in gamma-rays above 100 MeV of each blazar is used as the weight, since the blazars with higher flux are expected to emit more high-energy neutrinos (Murase et al. 2014; Petropoulou et al. 2015) and, therefore, are more likely to be the source of an alert neutrino. A similar weighting scheme was followed in a previous IceCube analysis using a different neutrino catalog (Huber 2019). The second weighting scheme utilizes the light curves from the Light Curve Repository[74] made available by the Fermi-LAT collaboration (Fermi Large Area Telescope Collaboration 2021). Here we use the normalized flux in the 1 month time bin that coincides with the neutrino arrival time as the weight, and thereby use the blazar's temporal information. This procedure is similar to the one

followed in Aartsen et al. (2018b). From the 2089 blazars selected for this analysis, 1161 had flux variability and were released in the light-curve repository. The weights are calculated as follows:

1. If the light curve of a blazar is not provided in the repository, it is assumed that it is not variable and the average energy flux is considered as the flux at the time of the neutrino's arrival.
2. If there is a flux measurement at the neutrino arrival time, it is used as the weight.
3. If there is no flux measurement in the time bin of the neutrino arrival or it is an upper limit, we check the monthly time bin before and after the time bin of the neutrino event (neighboring bins). If both have a flux measurement, the weight is an average of both. If only one of them has a measurement, the weight is equal to that flux. This assumes that the monthly energy flux does not vary greatly from one month to another.
4. If there is no flux measurement or only an upper limit is provided in the time bin of the neutrino event and its neighboring time bins, then a weight of zero is assigned. The weight is also set to zero when there are no measurements available in the neighboring bins. This avoids mixing the hypotheses for the two weighting schemes.

3.3. Radio Fundamental Catalog Sources

The second catalog we consider for coincidences with IceCat-1 is the Radio Fundamental Catalog (RFC), in its 2022a version.[75] It contains 20,499 objects detected between 1980 April 11 and 2022 March 24 at 22 GHz, 8.6 GHz, 5 GHz, and 2.2 GHz observed with very long baseline interferometry (VLBI) observations (Jennison 1958).

For the analysis presented here, we use the flux density integrated over VLBI images at 8.6 GHz as a weight and select AGNs with flux density $S_{8.6 \text{ GHz}} \geqslant 150$ mJy, which leaves a total of 3413 AGNs (828 in common with the subsample from 4LAC-DR2 described in the previous section). We follow the selection criteria applied in Plavin et al. (2020) with the purpose of cross-checking the results obtained in their analysis. The procedure followed to compare both methods is explained in the Appendix and discussed in Section 6. The AGNs from this catalog with the same selection criteria have also been analyzed as potential sources of astrophysical neutrinos at lower energies, with conflicting results; see Plavin et al. (2021) and Zhou & Kamionkowski (2021).

4. Analysis Technique

The statistical significance of the overall correlation between the neutrino alerts and various candidate source catalogs is calculated using the stacking analysis method. In this method, the hypothesis that we test is that the neutrino is correlated with a coincident source from the candidate source class. "Coincident" is defined here as the source lying within the 90% error contour of the reconstructed arrival direction of the neutrino. The null hypothesis is that the neutrino is not correlated with any sources, either because it is atmospheric background or because it comes from a source not included in the catalog

---
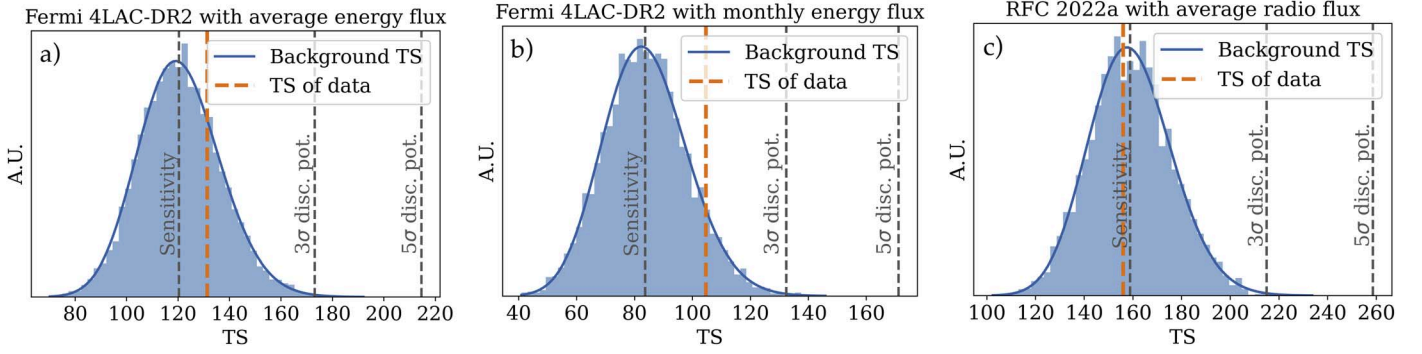
Figure 3. The blue histogram shows the distribution of the TS values for $N = 5000$ background maps, fitted to a gamma distribution (blue curve). The orange dotted line represents the observed TS of the data, while the gray lines represent the TS_{data} needed to reject the background hypothesis at the 3σ or 5σ level. Panel (a): for the Fermi 4LAC-DR2 catalog with the average energy flux weights, $TS_{data}= 131.3$, while $TS = 120.4$ for the median background maps, leading to a p-value of 0.248. Panel (b): for the Fermi 4LAC-DR2 catalog with the monthly energy flux weights, $TS_{data}= 104.6$, median background maps has $TS = 83.6$, and the p-value is 0.08. Panel (c): for the RFC 2022a catalog, $TS_{data}= 155.8$, $TS = 158.9$ for the median background maps, and the p-value is 0.57.

being tested. The likelihood $\mathscr{L}$ is the weighted sum of a signal PDF, S, and a background PDF, B,

$$\mathscr{L} = \frac{n_S}{N}S + \left(1 - \frac{n_S}{N}\right)B \qquad (1)$$

where n_S is the number of signal events and N is the total number of signal and background neutrino candidate events. The TS for a single neutrino i ($N = 1$) is defined as

$$TS_i = 2\log\left(\frac{\mathscr{L}(n_S = 1)}{\mathscr{L}(n_S = 0)}\right) = 2\log\frac{\hat{S}}{B}. \qquad (2)$$

Treating each neutrino independently, the hypothesis is tested for each coincident source b. The combination returning the highest TS is selected as the most likely counterpart. If $TS < 0$, the background hypothesis is chosen, i.e., $S/B = 1$. The signal PDF is defined as

$$S = S_{\text{signalness},\nu} \cdot S_{\text{spatial},\nu}(\boldsymbol{x}_b) \cdot w_b, \qquad (3)$$

where $S_{\text{signalness},\nu}$ is the signalness of the neutrino alert; $S_{\text{spatial},\nu}(\boldsymbol{x}_b)$ is the neutrino point-spread function, calculated using the re-scaled likelihood maps from the reconstruction of the alerts that depends on the position of the source $\boldsymbol{x}_b$ (see Section 3); and w_b is the source weight that depends on the hypothesis of the neutrino production mechanism. The most likely counterpart is then the source for which $S_{\text{spatial},\nu}(\boldsymbol{x}_b) \cdot w_b$ is maximum, which we denote in Equation (2) as $\hat{S}$. The signalness is a fixed parameter for each individual neutrino, so it does not affect the selection of the counterpart.

For the background case, in which the neutrino is not associated with any source, the probability of finding a correlation by chance can be assumed to be isotropic, and therefore the background PDF is simply defined by $B = B_{\text{spatial}} = \frac{1}{4\pi}$. Finally, the TS of the data is calculated by summing over all neutrino alerts, $TS_{data} = \sum_i TS_i$. To calculate the significance of the result, $N = 5000$ background pseudo-experiments are constructed by fixing the direction of the neutrino alerts and scrambling the candidate sources in R.A. and decl., while maintaining the high galactic latitude criterion from the Fermi 4LAC-DR2 catalog of $|b| > 10°$. Then the TS is calculated for each of the background maps, and its distribution is fitted to a gamma distribution for the p-value estimation.

For the analysis using Fermi-LAT 4LAC catalog with average flux weights, the sensitivity flux, which is defined as the neutrino flux needed in order to get a TS larger than the median of the background distribution in 90% of the cases, is at 5.1% of the astrophysical flux, which corresponds to 6.3 signal correlations from the 275 neutrinos in the IceCat-1 catalog, i.e., 6.3 neutrinos correlated with their sources. The sensitivity for the same catalog with the monthly energy flux weighting scheme (second analysis) is at 4.4% of the astrophysical flux, which is equivalent to 5.5 signal correlations. Using the RFC catalog and the average VLBI, the sensitivity flux is 6% of the astrophysical flux, or 7.4 signal correlations.

5. Results

5.1. Fermi 4LAC-DR2 with Average Energy Flux

No significant correlation was found between the 2089 selected blazars from Fermi 4LAC-DR2 weighted by the average 10 yr energy flux and the neutrino alerts, with a p-value of 0.248; see Figure 3, panel (a). The 10 most significant correlations (the 10 blazar-neutrino pairs with the highest TS_i in the data) are listed in Table 1. The two strongest correlations have been extensively studied (see Section 1, TXS 0506+056 —IC170922A and PKS 1502+106—IC190730A). The third and fourth correlation are also interesting since 3C 454.3 and Mkn 421 are two of the brightest sources in the sky, which explains the high TS, but in both cases the area of the error region of the associated neutrino is very large. The areas of the 90% uncertainty contours are 26.80 deg^2 and 56.07 deg^2, respectively, compared to the median 90% contour area of all alerts, which is 5.96 deg^2, or the 90% contour area of IC170922A and IC190730A, of 1.54 deg^2 and 5.61 deg^2, respectively.

5.2. Fermi 4LAC-DR2 with Monthly Energy Flux

The TS is again consistent with the null hypothesis when the selected blazars are weighted by the energy flux at the neutrino arrival time (see Figure 3, panel (b)). The p-value of this analysis is 0.08. Table 2 shows the 10 most contributing correlations to the TS. The main contribution to TS_{data} is given by TXS 0506 + 056 and IC170922A, since the blazar was flaring in gamma-rays at the neutrino arrival time, as mention in Section 1, leading to a higher TS value than observed in the analysis with average energy flux weights. On the other hand, one can see that the blazar 3C 454.3 was in a quiescent state at the neutrino arrival time, and therefore, the TS value of that

Table 1
The 10 Correlations that Contribute Most to the TS of the Data Using the Fermi 4LAC-DR2 Catalog and Average Flux Weights

Neutrino	Signalness	Blazar	d (deg)	TS
IC170922A	63 %	TXS 0506+056	0.11	7.43
IC190730A	67 %	PKS 1502+106	0.27	7.13
IC120523A	49 %	3C 454.3	0.72	7.12
IC111208A	45 %	Mkn 421	0.78	5.63
IC190704A	49 %	NVSS J104516+275136	1.04	5.14
IC190504A	39 %	NVSS J042025-374443	0.50	4.18
IC200109A	77 %	TXS 1100+122	0.36	4.05
IC181014A	39 %	PKS 1454-354	0.99	3.87
IC150104A	45 %	MG2 J180948+2910	0.50	3.41
IC130127A	61 %	PKS B2330-017	0.58	3.17

Note. The first column is the neutrino using the nomenclature of the realtime program; the second column is the signalness of each neutrino; the third column is the J2000 name of the most likely counterpart; the fourth column is the angular distance between the candidate source and the neutrino (calculated as the angle between the two sight lines); and the last column is the contribution of each correlation to the final TS.

Table 2
The 10 Correlations that Contribute Most to the TS of the Data Using the Fermi 4LAC-DR2 Catalog and Monthly Flux Weights

Neutrino	Signalness	Blazar	d (deg)	TS
IC170922A	63 %	TXS 0506+056	0.11	9.43
IC190730A	67 %	PKS 1502+106	0.27	5.63
IC111208A	45 %	Mkn 421	0.78	5.36
IC130125A	53 %	S5 0016+73	1.03	4.87
IC190504A	39 %	NVSS J042025-374443	0.50	4.41
IC150104A	49 %	MG2 J180948+2910	0.50	4.28
IC111216A	95 %	TXS 0222+185	0.51	4.13
IC200109A	78 %	TXS 1100+122	0.36	3.96
IC140101A	56 %	PMN J1243-0218	1.33	3.81
IC181014A	39 %	PKS 1454-354	0.99	3.54

Note. The first column is the neutrino using the nomenclature of the realtime program; the second column is the signalness of each neutrino; the third column is the J2000 name of the most likely counterpart; the fourth column is the angular distance between the candidate source and the neutrino (calculated as the angle between the two sight lines); and the last column is the contribution of each correlation to the final TS.

Table 3
The 10 Correlations that Contribute Most to the TS of the Data Using the RFC 2022a Catalog

Neutrino	Signalness	AGN	d (deg)	TS
IC120523A	49 %	J2253+1608	0.72	5.62
IC170922A	63 %	J0509+0541	0.12	5.41
IC190730A	67 %	J1504+1029	0.28	5.21
IC150812A	83 %	J2151+0552	0.47	4.12
IC141110A	29 %	J1652+0618	0.26	3.51
IC150428A	32 %	J0204+1514	0.44	3.48
IC130125A	53 %	J0019+7327	1.02	3.19
IC170422A	39 %	J1550+0527	3.29	3.05
IC140307A	40 %	J2025+3343	1.67	3.02
IC200530A	59 %	J1659+2629	0.48	2.99

Note. The first column is the neutrino using the nomenclature of the realtime program; the second column is the signalness of each neutrino; the third column is the J2000 name of the most likely AGN counterpart; the fourth column is the angular distance between the candidate source and the neutrino; and the last column is the contribution of each correlation to the final TS.

correlation is low and is not within the 10 most contributing ones.

5.3. RFC 2022 with Average VLBI Flux

The result from this third analysis, shown in Figure 3, panel (c), using the RFC catalog and the average VLBI flux at 8.6 GHz as weight for the contribution of the AGNs is that the data is compatible with the null hypothesis, with a *p*-value of 0.57. In Table 3 the 10 correlations with the highest TS are shown. It is worth noting that the correlations of TXS 0506 + 056 with IC170922A and PKS 1502 + 106 with IC190730A appear on the list (with the nomenclature used in the RFC catalog for the AGNs), since they are both very bright in radio as well.

6. Discussion and Conclusions

In this paper we have described a new method developed within IceCube that allows us to calculate the overall correlation between neutrino alerts and a catalog of candidate sources. We conducted three analyses: two searching for correlations with blazars from Fermi 4LAC-DR2 catalog and one with AGNs from the RFC 2022a catalog. A significant correlation was not found in any of the three cases, meaning that the majority of the neutrino alerts are neither produced in bright or flaring gamma-ray blazars nor in radio-bright AGNs.

The analyses presented here, and the method itself, rely heavily on the robustness of the reconstruction. Due to the way the contours are calculated, which determines how broad the neutrino spatial PDF is, a better handle on the systematic uncertainties is crucial. The reconstruction method used in IceCube's realtime system is being improved, and further modifications will be implemented in the future (Abbasi et al. 2021b), which might give an opportunity to revisit this analysis with improved sensitivity.

The results obtained in this paper are, however, compatible with previous hints of a signal, e.g., Aartsen et al. (2018b) and Rodrigues et al. (2021). The expected number of chance correlations that have $TS_i > 7$ is 0.077 for the 4LAC-DR2 catalog weighted by the average energy flux. In data, there are three such correlations, which point to a potential signal being present but nondiscernible from chance coincidences. The observed TS_{data} is compatible with the TS distribution that one would obtain if only 1% of the blazars in the selected Fermi 4LAC-DR2 catalog emits neutrinos. This is calculated by randomly choosing 1% of sources in multiple pseudo-experiments and injecting them as signal, i.e., the location of the blazar is moved into the error region of a neutrino so that a correlation is forced. The same study was performed with RFC 2022a, with similar results. This indicates the possibility that only a small fraction of the gamma-ray bright and radio-bright AGN population are sources of high-energy neutrinos.

The third correlation analysis was designed to be similar to Plavin et al. (2020) and allows for comparison. Adding more neutrino events and additional information, such as the signalness or the spatial PDF from the reconstruction, leads to a TS_{data} compatible with the background. Even when the definition of "coincidence" resembles the one in their paper (i.e., when the spatial term of the signal PDF is simplified to a uniform distribution inside of the error contour), we do not observe the same significance. Details of these cross-checks can be found in the Appendix.

The possibility of testing several hypotheses for the search of correlations with neutrino realtime alerts is the main strength of the method that was developed and explained in this paper. The information from the realtime reconstruction algorithm and the signalness of the alert allow us to be more sensitive to potential signal, and they were used for the first time in an analysis for the results presented here.

Appendix
Comparisons to Published Analyses

Plavin et al. (2020) found a 3σ correlation between 56 IceCube high-energy neutrinos and a previous version of the Astrogeo catalog[76]. Using the same selection criteria for the candidate sources, we repeat this analysis with a few changes to the method, including more of the available information.

One of the key differences is the definition of the TS, which, in Plavin et al.'s (2020) analysis, is simply the geometric

---

[76] http://astrogeo.org/sol/rfc/rfc_2019c/

average of the VLBI flux of the sources coincident with the neutrinos. Their neutrino selection consists of alert and alert-like events from different catalogs published by IceCube, and a table with the full catalog is included along with their paper. They are chosen so that only high-energy ($E > 200$ TeV) tracks with good angular resolution ($\Omega_{90} < 10 \deg^2$) are included in the catalog. Fifty-six events from 2009–2019 pass their criteria, 44 of which are also contained in the IceCat-1 catalog. Of the remaining 12 events, 10 are from the period from 2009–2011, which was not included in the IceCat-1 catalog, and two did not pass our current alert criteria.

For comparison, our definition of the TS is maintained, but the spatial term in the signal PDF is calculated as in Plavin et al. (2020). The information that IceCube publishes in the GCN Circular whenever an alert is detected is the reconstructed direction along with the minimum rectangle that encapsulates the 90% error contour in R.A. and decl. (see Figure 1). In Plavin et al. (2020), the coordinate-wise errors are multiplied by the ratio of the 90% quantiles of 2D and 1D Gaussian distributions (≈ 1.3). An extra parameter x is added linearly in all directions to account for possible unknown systematic uncertainties. It varies from $0°$–$1°$ in increments of $0°.1$ and fitted to find the minimum pre-trial p-value, which is obtained at $x = 0°.5$ in Plavin et al. (2020). Finally, the error region is assumed to be composed of four points joint by elliptical segments. This is shown in Figure 4.

IceCube already calculates the errors by assuming a 2D distribution, but the extra 1.3 factor is also applied in the comparison for consistency with Plavin et al. (2020). Systematic uncertainties are added to the contours before publishing them, although one could argue that there are unknown systematics. This is currently being studied (see, e.g., Abbasi et al. 2021b), but the method to calibrate the errors is conservative, and the real uncertainties could be smaller. However, it is worth investigating this scaling up of the contours since other analyses have also found interesting hints of signals following a similar procedure (although in some cases with a very different neutrino data sample focused on lower energies; e.g., Giommi et al. 2020; Buson et al. 2022).

For the comparison analysis, we switch the spatial term of the signal PDF from the neutrino point-spread function (based on the reconstruction's likelihood landscape) to the simpler coincidence-based function described above, multiplying the angular errors by 1.3 and considering the added $0°.5$ as a fixed value. Then the $S_{spatial}$ is 1 for all AGNs inside the area of the calculated contour and 0 outside. This is performed with the data sets described in Section 3 (IceCat-1 catalog + RFC 2022a) and the original data set from Plavin et al. (2020; 56 alert and alert-like events + RFC 2019c) with and without the scaling factors, 1.3 from the quantiles + $0°.5$ for systematic uncertainties. Without scaling, the error bars would be similar to those in Figure 4, panel (b), while for the scaled-up contours, the error bars would be as in Figure 4, panel (d). For the neutrinos from the 56 alert and alert-like event catalog that do not have a signalness, a signalness of 45.1% is assumed, which is the average of the IceCat-1 catalog.

The results can be seen in Table 4. The lowest p-value is achieved with the test that is the most similar to Plavin et al. (2020; the same AGN and neutrino catalogs and scaling of the angular uncertainty). However, when more events are added, the significance drops. The same happens when the angular errors are not scaled up, which indicates that the correlations
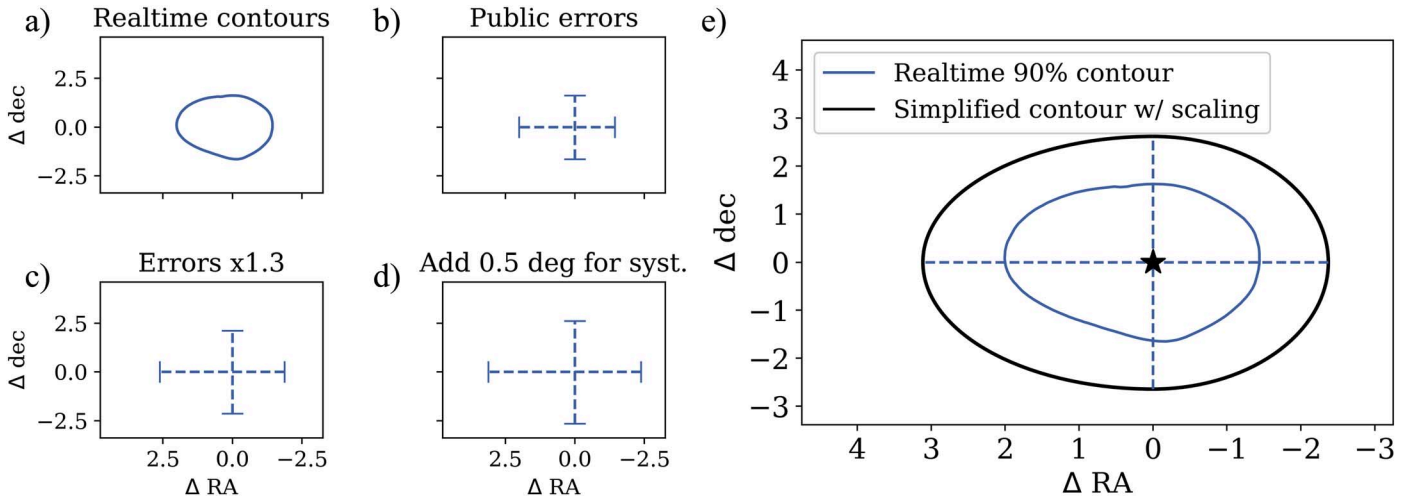
Figure 4. Example of the simplification and scaling that are applied to the realtime contours in Plavin et al. (2020), which is also done in the cross-check presented here. From the original contours in panel (a), only the minimum rectangle is published, which is translated to uncertainty in the coordinates (panel (b)). Those errors are multiplied by 1.3 (panel (c)), and an extra parameter is added to account for systematic uncertainties, leading to a minimum p-value at an added 0°.5 (panel (d)). The error bars are joined by elliptical segments to obtain the simplified contours corresponding to the best-fit position from the reconstruction, represented by the black star (panel (e)).

Table 4
Results from the Cross-checks to Plavin et al. (2020)

Check		p-value	Significance
RFC 2022a + IceCat-1	With scaling	0.048	1.67
	Without scaling	0.32	0.47
RFC 2019c + Alert-like events	With scaling	0.0043	2.63
	Without scaling	0.2	0.84

that are contributing to the TS are from AGNs that are from outside the original contours, and therefore are far away from the best-fit position.

Only one of the four correlations that drive the result in Plavin et al. (2020) appears in Table 3, as well as in the two tests with the RFC 2019c + alert-like events selection, due to its high signalness and the brightness of the AGN. The four most significant correlations from Plavin et al. (2020) are found in the test of RFC 2019c + alert-like events including scaling as expected, since this is the test that is closest to their analysis. With the information available, we cannot confirm the findings of Plavin et al. (2020), and the only hint of excess disappears when we use a more sophisticated description of the spatial probability density function for the neutrino events.

ORCID iDs

R. Abbasi ⓘ https://orcid.org/0000-0001-6141-4205
M. Ackermann ⓘ https://orcid.org/0000-0001-8952-588X
S. K. Agarwalla ⓘ https://orcid.org/0000-0002-9714-8866
J. A. Aguilar ⓘ https://orcid.org/0000-0003-2252-9514
M. Ahlers ⓘ https://orcid.org/0000-0003-0709-5631
J. M. Alameddine ⓘ https://orcid.org/0000-0002-9534-9189
G. Anton ⓘ https://orcid.org/0000-0003-2039-4724
C. Argüelles ⓘ https://orcid.org/0000-0003-4186-4182
Y. Ashida ⓘ https://orcid.org/0000-0003-4136-2086
S. N. Axani ⓘ https://orcid.org/0000-0001-8866-3826
X. Bai ⓘ https://orcid.org/0000-0002-1827-9121
A. Balagopal V. ⓘ https://orcid.org/0000-0001-5367-8876
S. W. Barwick ⓘ https://orcid.org/0000-0003-2050-6714
V. Basu ⓘ https://orcid.org/0000-0002-9528-2009

J. J. Beatty ⓘ https://orcid.org/0000-0003-0481-4952
J. Becker Tjus ⓘ https://orcid.org/0000-0002-1748-7367
J. Beise ⓘ https://orcid.org/0000-0002-7448-4189
C. Bellenghi ⓘ https://orcid.org/0000-0001-8525-7515
S. BenZvi ⓘ https://orcid.org/0000-0001-5537-4710
E. Bernardini ⓘ https://orcid.org/0000-0003-3108-1141
D. Z. Besson ⓘ https://orcid.org/0000-0001-6733-963X
E. Blaufuss ⓘ https://orcid.org/0000-0001-5450-1757
S. Blot ⓘ https://orcid.org/0000-0003-1089-3001
J. Y. Book ⓘ https://orcid.org/0000-0001-6687-5959
C. Boscolo Meneguolo ⓘ https://orcid.org/0000-0001-8325-4329
S. Böser ⓘ https://orcid.org/0000-0002-5918-4890
O. Botner ⓘ https://orcid.org/0000-0001-8588-7306
J. Böttcher ⓘ https://orcid.org/0000-0002-3387-4236
B. Brinson ⓘ https://orcid.org/0000-0001-9128-1159
M. A. Campana ⓘ https://orcid.org/0000-0003-4162-5739
C. Chen ⓘ https://orcid.org/0000-0002-8139-4106
Z. Chen ⓘ https://orcid.org/0000-0002-2813-7688
D. Chirkin ⓘ https://orcid.org/0000-0003-4911-1345
B. A. Clark ⓘ https://orcid.org/0000-0003-4089-2245
A. Coleman ⓘ https://orcid.org/0000-0003-1510-1712
J. M. Conrad ⓘ https://orcid.org/0000-0002-6393-0438
P. Coppin ⓘ https://orcid.org/0000-0001-6869-1280
P. Correa ⓘ https://orcid.org/0000-0002-1158-6735
D. F. Cowen ⓘ https://orcid.org/0000-0003-4738-0787
P. Dave ⓘ https://orcid.org/0000-0002-3879-5115
C. De Clercq ⓘ https://orcid.org/0000-0001-5266-7059
J. J. DeLaunay ⓘ https://orcid.org/0000-0001-5229-1995
D. Delgado ⓘ https://orcid.org/0000-0002-4306-8828
H. Dembinski ⓘ https://orcid.org/0000-0003-3337-3850
A. Desai ⓘ https://orcid.org/0000-0001-7405-9994
P. Desiati ⓘ https://orcid.org/0000-0001-9768-1858
K. D. de Vries ⓘ https://orcid.org/0000-0002-9842-4068
G. de Wasseige ⓘ https://orcid.org/0000-0002-1010-5100
T. DeYoung ⓘ https://orcid.org/0000-0003-4873-3783
A. Diaz ⓘ https://orcid.org/0000-0001-7206-8336
J. C. Díaz-Vélez ⓘ https://orcid.org/0000-0002-0087-0693
H. Dujmovic ⓘ https://orcid.org/0000-0003-1891-0718
M. A. DuVernois ⓘ https://orcid.org/0000-0002-2987-9691

P. Eller https://orcid.org/0000-0001-6354-5209
H. Erpenbeck https://orcid.org/0000-0001-6319-2108
P. A. Evenson https://orcid.org/0000-0001-7929-810X
K. L. Fan https://orcid.org/0000-0002-8246-4751
A. R. Fazely https://orcid.org/0000-0002-6907-8020
A. Fedynitch https://orcid.org/0000-0003-2837-3477
C. Finley https://orcid.org/0000-0003-3350-390X
L. Fischer https://orcid.org/0000-0002-7645-8048
D. Fox https://orcid.org/0000-0002-3714-672X
A. Franckowiak https://orcid.org/0000-0002-5605-2219
T. K. Gaisser https://orcid.org/0000-0003-4717-6620
E. Ganster https://orcid.org/0000-0003-4393-6944
A. Garcia https://orcid.org/0000-0002-8186-2459
A. Ghadimi https://orcid.org/0000-0002-6350-6485
C. Glaser https://orcid.org/0000-0001-5998-2553
T. Glauch https://orcid.org/0000-0003-1804-4055
T. Glüsenkamp https://orcid.org/0000-0002-2268-9297
S. Goswami https://orcid.org/0000-0002-0373-9770
S. J. Gray https://orcid.org/0000-0003-2907-8306
S. Griffin https://orcid.org/0000-0002-0779-9623
S. Griswold https://orcid.org/0000-0002-7321-7513
P. Gutjahr https://orcid.org/0000-0001-7980-7285
A. Hallgren https://orcid.org/0000-0001-7751-4489
L. Halve https://orcid.org/0000-0003-2237-6714
F. Halzen https://orcid.org/0000-0001-6224-2417
H. Hamdaoui https://orcid.org/0000-0001-5709-2100
A. Haungs https://orcid.org/0000-0002-9638-7574
K. Helbing https://orcid.org/0000-0003-2072-4172
F. Henningsen https://orcid.org/0000-0002-0680-6588
N. Heyer https://orcid.org/0000-0001-9036-8623
C. Hill https://orcid.org/0000-0003-0647-9174
W. Hou https://orcid.org/0000-0003-3422-7185
T. Huber https://orcid.org/0000-0002-6515-1673
K. Hultqvist https://orcid.org/0000-0003-0602-9472
M. Hünnefeld https://orcid.org/0000-0002-2827-6522
G. S. Japaridze https://orcid.org/0000-0002-7000-5291
M. Jin https://orcid.org/0000-0003-0487-5595
B. J. P. Jones https://orcid.org/0000-0003-3400-8986
D. Kang https://orcid.org/0000-0002-5149-9767
W. Kang https://orcid.org/0000-0003-3980-3778
A. Kappes https://orcid.org/0000-0003-1315-3711
T. Karg https://orcid.org/0000-0003-3251-2126
M. Karl https://orcid.org/0000-0003-2475-8951
A. Karle https://orcid.org/0000-0001-9889-5161
U. Katz https://orcid.org/0000-0002-7063-4418
M. Kauer https://orcid.org/0000-0003-1830-9076
J. L. Kelley https://orcid.org/0000-0002-0846-4542
A. Khatee Zathul https://orcid.org/0000-0002-8735-8579
A. Kheirandish https://orcid.org/0000-0001-7074-0539
J. Kiryluk https://orcid.org/0000-0003-0264-3133
S. R. Klein https://orcid.org/0000-0003-2841-6553
A. Kochocki https://orcid.org/0000-0003-3782-0128
R. Koirala https://orcid.org/0000-0002-7735-7169
H. Kolanoski https://orcid.org/0000-0003-0435-2524
T. Kontrimas https://orcid.org/0000-0001-8585-0933
L. Köpke https://orcid.org/0000-0001-8530-6348
C. Kopper https://orcid.org/0000-0001-6288-7637
D. J. Koskinen https://orcid.org/0000-0002-0514-5917
P. Koundal https://orcid.org/0000-0002-5917-5230
M. Kovacevich https://orcid.org/0000-0002-5019-5745
M. Kowalski https://orcid.org/0000-0001-8594-8666
A. Kumar https://orcid.org/0000-0002-8367-8401

N. Kurahashi https://orcid.org/0000-0003-1047-8094
C. Lagunas Gualda https://orcid.org/0000-0002-9040-7191
M. Lamoureux https://orcid.org/0000-0002-8860-5826
M. J. Larson https://orcid.org/0000-0002-6996-1155
F. Lauber https://orcid.org/0000-0001-5648-5930
J. P. Lazar https://orcid.org/0000-0003-0928-5025
J. W. Lee https://orcid.org/0000-0001-5681-4941
K. Leonard DeHolton https://orcid.org/0000-0002-8795-0601
A. Leszczyńska https://orcid.org/0000-0003-0935-6313
M. Lincetto https://orcid.org/0000-0002-1460-3369
Q. R. Liu https://orcid.org/0000-0003-3379-6423
E. Lohfink https://orcid.org/0000-0003-3248-5682
L. Lu https://orcid.org/0000-0003-3175-7770
F. Lucarelli https://orcid.org/0000-0002-9558-8788
A. Ludwig https://orcid.org/0000-0001-9038-4375
W. Luszczak https://orcid.org/0000-0003-3085-0674
Y. Lyu https://orcid.org/0000-0002-2333-4383
J. Madsen https://orcid.org/0000-0003-2415-9959
I. C. Mariş https://orcid.org/0000-0002-5771-1124
R. Maruyama https://orcid.org/0000-0003-2794-512X
F. Mayhew https://orcid.org/0000-0001-7609-403X
F. McNally https://orcid.org/0000-0002-0785-2244
K. Meagher https://orcid.org/0000-0003-3967-1533
M. Meier https://orcid.org/0000-0002-9483-9450
L. Merten https://orcid.org/0000-0003-1332-9895
T. Montaruli https://orcid.org/0000-0001-5014-2152
R. W. Moore https://orcid.org/0000-0003-4160-4700
M. Moulai https://orcid.org/0000-0001-7909-5812
R. Naab https://orcid.org/0000-0003-2512-466X
R. Nagai https://orcid.org/0000-0001-7503-2777
J. Necker https://orcid.org/0000-0003-0280-7484
H. Niederhausen https://orcid.org/0000-0002-9566-4904
M. U. Nisa https://orcid.org/0000-0002-6859-3944
S. C. Nowicki https://orcid.org/0000-0003-2497-8057
A. Obertacke Pollmann https://orcid.org/0000-0002-2492-043X
B. Oeyen https://orcid.org/0000-0003-2940-3164
E. O'Sullivan https://orcid.org/0000-0003-1882-8802
H. Pandya https://orcid.org/0000-0002-6138-4808
N. Park https://orcid.org/0000-0002-4282-736X
E. N. Paudel https://orcid.org/0000-0001-9276-7994
C. Pérez de los Heros https://orcid.org/0000-0002-2084-5866
J. Peterson https://orcid.org/0000-0002-7985-1443
S. Philippen https://orcid.org/0000-0002-0276-0092
A. Pizzuto https://orcid.org/0000-0002-8466-8168
M. Plum https://orcid.org/0000-0001-8691-242X
B. Pries https://orcid.org/0000-0003-4811-9863
A. Rehman https://orcid.org/0000-0001-7616-5790
P. Reichherzer https://orcid.org/0000-0003-4513-8241
E. Resconi https://orcid.org/0000-0003-0705-2770
S. Reusch https://orcid.org/0000-0002-7788-628X
W. Rhode https://orcid.org/0000-0003-2636-5000
B. Riedel https://orcid.org/0000-0002-9524-8943
M. Rongen https://orcid.org/0000-0002-7057-1007
C. Rott https://orcid.org/0000-0002-6958-6033
D. Ryckbosch https://orcid.org/0000-0002-8759-7553
I. Safa https://orcid.org/0000-0001-8737-6825
D. Salazar-Gallegos https://orcid.org/0000-0002-9312-9684
A. Sandrock https://orcid.org/0000-0002-6779-1172
M. Santander https://orcid.org/0000-0001-7297-8217

S. Sarkar ⓘ https://orcid.org/0000-0002-1206-4330
S. Sarkar ⓘ https://orcid.org/0000-0002-3542-858X
H. Schieler ⓘ https://orcid.org/0000-0002-2637-4778
S. Schindler ⓘ https://orcid.org/0000-0001-5507-8890
F. Schlüter ⓘ https://orcid.org/0000-0002-5545-4363
J. Schneider ⓘ https://orcid.org/0000-0001-7752-5700
F. G. Schröder ⓘ https://orcid.org/0000-0001-8495-7210
L. Schumacher ⓘ https://orcid.org/0000-0001-8945-6722
S. Sclafani ⓘ https://orcid.org/0000-0001-9446-1219
S. Seunarine ⓘ https://orcid.org/0000-0003-3272-6896
A. Sharma ⓘ https://orcid.org/0000-0001-5397-6777
M. Silva ⓘ https://orcid.org/0000-0001-6940-8184
B. Skrzypek ⓘ https://orcid.org/0000-0002-0910-1057
B. Smithers ⓘ https://orcid.org/0000-0003-1273-985X
J. Soedingrekso ⓘ https://orcid.org/0000-0003-1011-2797
D. Soldin ⓘ https://orcid.org/0000-0003-3005-7879
G. Sommani ⓘ https://orcid.org/0000-0002-0094-826X
G. M. Spiczak ⓘ https://orcid.org/0000-0002-0030-0519
C. Spiering ⓘ https://orcid.org/0000-0001-7372-0074
T. Stezelberger ⓘ https://orcid.org/0000-0003-2676-9574
T. Stuttard ⓘ https://orcid.org/0000-0001-7944-279X
G. W. Sullivan ⓘ https://orcid.org/0000-0002-2585-2352
I. Taboada ⓘ https://orcid.org/0000-0003-3509-3457
S. Ter-Antonyan ⓘ https://orcid.org/0000-0002-5788-1369
W. G. Thompson ⓘ https://orcid.org/0000-0003-2988-7998
J. Thwaites ⓘ https://orcid.org/0000-0001-9179-3760
K. Tollefson ⓘ https://orcid.org/0000-0001-9725-1479
S. Toscano ⓘ https://orcid.org/0000-0002-1860-2240
A. Trettin ⓘ https://orcid.org/0000-0003-0350-3597
C. F. Tung ⓘ https://orcid.org/0000-0001-6920-7841
M. A. Unland Elorrieta ⓘ https://orcid.org/0000-0002-6124-3255
N. Valtonen-Mattila ⓘ https://orcid.org/0000-0002-1830-098X
J. Vandenbroucke ⓘ https://orcid.org/0000-0002-9867-6548
N. van Eijndhoven ⓘ https://orcid.org/0000-0001-5558-3328
J. van Santen ⓘ https://orcid.org/0000-0002-2412-9728
S. Verpoest ⓘ https://orcid.org/0000-0002-3031-3206
C. Walck ⓘ https://orcid.org/0000-0002-4188-9219
T. B. Watson ⓘ https://orcid.org/0000-0002-8631-2253
C. Weaver ⓘ https://orcid.org/0000-0003-2385-2559

J. Weldert ⓘ https://orcid.org/0000-0002-3709-2354
C. Wendt ⓘ https://orcid.org/0000-0001-8076-8877
N. Whitehorn ⓘ https://orcid.org/0000-0002-3157-0407
C. H. Wiebusch ⓘ https://orcid.org/0000-0002-6418-3008
M. Wolf ⓘ https://orcid.org/0000-0001-9991-3923
S. Yoshida ⓘ https://orcid.org/0000-0003-2480-5105
T. Yuan ⓘ https://orcid.org/0000-0002-7041-5872
Z. Zhang ⓘ https://orcid.org/0000-0002-7347-283X

References

Aartsen, M. G., Abbasi, R., Ackermann, M., et al. 2014, JInst, 9, P03009
Aartsen, M. G., Ackermann, M., Adams, J., et al. 2017a, JInst, 12, P03012
Aartsen, M. G., Ackermann, M., Adams, J., et al. 2017b, APh, 92, 30
Aartsen, M. G., Ackermann, M., Adams, J., et al. 2018a, Sci, 361, 147
Aartsen, M. G., Ackermann, M., Adams, J., et al. 2018b, Sci, 361, eaat1378
Abbasi, R., Abdou, Y., Abu-Zayyad, T., et al. 2010, NIMPA, 618, 139
Abbasi, R., Ackermann, M., Adams, J., et al. 2009, NIMPA, 601, 294
Abbasi, R., Ackermann, M., Adams, J., et al. 2022a, Sci, 378, 538
Abbasi, R., Ackermann, M., Adams, J., et al. 2022b, PhRvD, 106, 022005
Abbasi, R., Ackermann, M., Adams, J., et al. 2022c, ApJ, 928, 50
Abbasi, R., Ackermann, M., Adams, J., et al. 2023, arXiv:2304.01174
Abbasi, R., Ackermann, M., Adams, J., et al. 2021a, JInst, 16, P08034
Abbasi, R., Ackermann, M., Adams, J., et al. 2021b, ICRC (Berlin), 395, 1045
Ajello, M., Angioni, R., Axelsson, M., et al. 2020, ApJ, 892, 105
Blaufuss, E., Kintscher, T., Lu, L., & Tung, C. F. 2019, ICRC (Madison), 358, 1021
Buson, S., Tramacere, A., Pfeiffer, L., et al. 2022, ApJL, 933, L43
Fermi Large Area Telescope Collaboration 2021, ATel, 15110, 1
Giommi, P., Glauch, T., Padovani, P., et al. 2020, MNRAS, 497, 865
Gorski, K. M., Hivon, E., Banday, A. J., et al. 2005, ApJ, 622, 759
Haack, C., & Wiebusch, C. 2017, ICRC (Busan), 301, 1005
Huber, M. 2019, ICRC (Madison), 358, 916
Jennison, R. C. 1958, MNRAS, 118, 276
Lott, B., Gasparrini, D., & Ciprini, S. 2020, arXiv:2010.08406
Murase, K., Inoue, Y., & Dermer, C. D. 2014, PhRvD, 90, 023007
Murase, K., & Stecker, F. W. 2022, arXiv:2202.03381
Oikonomou, F., Petropoulou, M., Murase, K., et al. 2021, JCAP, 10, 082
Petropoulou, M., Dimitrakoudis, S., Padovani, P., Mastichiadis, A., & Resconi, E. 2015, MNRAS, 448, 2412
Plavin, A. V., Kovalev, Y. Y., Kovalev, Y. A., & Troitsky, S. V. 2020, ApJ, 894, 101
Plavin, A. V., Kovalev, Y. Y., Kovalev, Y. A., & Troitsky, S. V. 2021, ApJ, 908, 157
Rodrigues, X., Garrappa, S., Gao, S., et al. 2021, ApJ, 912, 54
Zhou, B., Kamionkowski, M., & feng Liang, Y. 2021, PhRvD, 103, 123018